

Conhecimentos pedagógicos e conteúdos disciplinares

das ciências exatas e da terra



Conhecimentos pedagógicos e conteúdos disciplinares

das ciências exatas e da terra



Editora chefe

Profª Drª Antonella Carvalho de Oliveira

Assistentes editoriais

Natalia Oliveira

Flávia Roberta Barão

Bibliotecária

Janaina Ramos

Projeto gráfico

Natália Sandrini de Azevedo

Camila Alves de Cremona

Luiza Alves Batista

Maria Alice Pinheiro

Imagens da capa

iStock

Edição de arte

Luiza Alves Batista

Revisão

Os autores

2021 by Atena Editora

Copyright © Atena Editora

Copyright do Texto © 2021 Os autores

Copyright da Edição © 2021 Atena Editora

Direitos para esta edição cedidos à Atena Editora pelos autores.

Open access publication by Atena Editora



Todo o conteúdo deste livro está licenciado sob uma Licença de Atribuição Creative Commons. Atribuição-Não-Comercial-NãoDerivativos 4.0 Internacional (CC BY-NC-ND 4.0).

O conteúdo dos artigos e seus dados em sua forma, correção e confiabilidade são de responsabilidade exclusiva dos autores, inclusive não representam necessariamente a posição oficial da Atena Editora. Permitido o *download* da obra e o compartilhamento desde que sejam atribuídos créditos aos autores, mas sem a possibilidade de alterá-la de nenhuma forma ou utilizá-la para fins comerciais.

Todos os manuscritos foram previamente submetidos à avaliação cega pelos pares, membros do Conselho Editorial desta Editora, tendo sido aprovados para a publicação com base em critérios de neutralidade e imparcialidade acadêmica.

A Atena Editora é comprometida em garantir a integridade editorial em todas as etapas do processo de publicação, evitando plágio, dados ou resultados fraudulentos e impedindo que interesses financeiros comprometam os padrões éticos da publicação. Situações suspeitas de má conduta científica serão investigadas sob o mais alto padrão de rigor acadêmico e ético.

Conselho Editorial

Ciências Humanas e Sociais Aplicadas

Prof. Dr. Alexandre Jose Schumacher – Instituto Federal de Educação, Ciência e Tecnologia do Paraná

Prof. Dr. Américo Junior Nunes da Silva – Universidade do Estado da Bahia

Profª Drª Andréa Cristina Marques de Araújo – Universidade Fernando Pessoa

Prof. Dr. Antonio Carlos Frasson – Universidade Tecnológica Federal do Paraná

Prof. Dr. Antonio Gasparetto Júnior – Instituto Federal do Sudeste de Minas Gerais

Prof. Dr. Antonio Isidro-Filho – Universidade de Brasília

Prof. Dr. Arnaldo Oliveira Souza Júnior – Universidade Federal do Piauí
Prof. Dr. Carlos Antonio de Souza Moraes – Universidade Federal Fluminense
Prof. Dr. Crisóstomo Lima do Nascimento – Universidade Federal Fluminense
Profª Drª Cristina Gaio – Universidade de Lisboa
Prof. Dr. Daniel Richard Sant'Ana – Universidade de Brasília
Prof. Dr. Deyvison de Lima Oliveira – Universidade Federal de Rondônia
Profª Drª Dilma Antunes Silva – Universidade Federal de São Paulo
Prof. Dr. Edvaldo Antunes de Farias – Universidade Estácio de Sá
Prof. Dr. Elson Ferreira Costa – Universidade do Estado do Pará
Prof. Dr. Eloi Martins Senhora – Universidade Federal de Roraima
Prof. Dr. Gustavo Henrique Cepolini Ferreira – Universidade Estadual de Montes Claros
Prof. Dr. Humberto Costa – Universidade Federal do Paraná
Profª Drª Ivone Goulart Lopes – Istituto Internazionele delle Figlie de Maria Ausiliatrice
Prof. Dr. Jadson Correia de Oliveira – Universidade Católica do Salvador
Prof. Dr. José Luis Montesillo-Cedillo – Universidad Autónoma del Estado de México
Prof. Dr. Julio Candido de Meirelles Junior – Universidade Federal Fluminense
Profª Drª Lina Maria Gonçalves – Universidade Federal do Tocantins
Prof. Dr. Luis Ricardo Fernandes da Costa – Universidade Estadual de Montes Claros
Profª Drª Natiéli Piovesan – Instituto Federal do Rio Grande do Norte
Prof. Dr. Marcelo Pereira da Silva – Pontifícia Universidade Católica de Campinas
Profª Drª Maria Luzia da Silva Santana – Universidade Federal de Mato Grosso do Sul
Prof. Dr. Miguel Rodrigues Netto – Universidade do Estado de Mato Grosso
Prof. Dr. Pablo Ricardo de Lima Falcão – Universidade de Pernambuco
Profª Drª Paola Andressa Scortegagna – Universidade Estadual de Ponta Grossa
Profª Drª Rita de Cássia da Silva Oliveira – Universidade Estadual de Ponta Grossa
Prof. Dr. Rui Maia Diamantino – Universidade Salvador
Prof. Dr. Saulo Cerqueira de Aguiar Soares – Universidade Federal do Piauí
Prof. Dr. Urandi João Rodrigues Junior – Universidade Federal do Oeste do Pará
Profª Drª Vanessa Bordin Viera – Universidade Federal de Campina Grande
Profª Drª Vanessa Ribeiro Simon Cavalcanti – Universidade Católica do Rio de Janeiro
Prof. Dr. William Cleber Domingues Silva – Universidade Federal Rural do Rio de Janeiro
Prof. Dr. Willian Douglas Guilherme – Universidade Federal do Tocantins

Ciências Agrárias e Multidisciplinar

Prof. Dr. Alexandre Igor Azevedo Pereira – Instituto Federal Goiano
Prof. Dr. Arinaldo Pereira da Silva – Universidade Federal do Sul e Sudeste do Pará
Prof. Dr. Antonio Pasqualetto – Pontifícia Universidade Católica de Goiás
Profª Drª Carla Cristina Bauermann Brasil – Universidade Federal de Santa Maria
Prof. Dr. Cleberton Correia Santos – Universidade Federal da Grande Dourados
Profª Drª Diocléa Almeida Seabra Silva – Universidade Federal Rural da Amazônia
Prof. Dr. Écio Souza Diniz – Universidade Federal de Viçosa
Prof. Dr. Fábio Steiner – Universidade Estadual de Mato Grosso do Sul
Prof. Dr. Fágner Cavalcante Patrocínio dos Santos – Universidade Federal do Ceará
Profª Drª Girlene Santos de Souza – Universidade Federal do Recôncavo da Bahia
Prof. Dr. Jael Soares Batista – Universidade Federal Rural do Semi-Árido
Prof. Dr. Jayme Augusto Peres – Universidade Estadual do Centro-Oeste
Prof. Dr. Júlio César Ribeiro – Universidade Federal Rural do Rio de Janeiro
Profª Drª Lina Raquel Santos Araújo – Universidade Estadual do Ceará
Prof. Dr. Pedro Manuel Villa – Universidade Federal de Viçosa
Profª Drª Raissa Rachel Salustriano da Silva Matos – Universidade Federal do Maranhão
Prof. Dr. Ronilson Freitas de Souza – Universidade do Estado do Pará
Profª Drª Talita de Santos Matos – Universidade Federal Rural do Rio de Janeiro

Prof. Dr. Tiago da Silva Teófilo – Universidade Federal Rural do Semi-Árido
Prof. Dr. Valdemar Antonio Paffaro Junior – Universidade Federal de Alfenas

Ciências Biológicas e da Saúde

Prof. Dr. André Ribeiro da Silva – Universidade de Brasília
Profª Drª Anelise Levay Murari – Universidade Federal de Pelotas
Prof. Dr. Benedito Rodrigues da Silva Neto – Universidade Federal de Goiás
Profª Drª Daniela Reis Joaquim de Freitas – Universidade Federal do Piauí
Profª Drª Débora Luana Ribeiro Pessoa – Universidade Federal do Maranhão
Prof. Dr. Douglas Siqueira de Almeida Chaves – Universidade Federal Rural do Rio de Janeiro
Prof. Dr. Edson da Silva – Universidade Federal dos Vales do Jequitinhonha e Mucuri
Profª Drª Elizabeth Cordeiro Fernandes – Faculdade Integrada Medicina
Profª Drª Eleuza Rodrigues Machado – Faculdade Anhanguera de Brasília
Profª Drª Elane Schwinden Prudêncio – Universidade Federal de Santa Catarina
Profª Drª Eysler Gonçalves Maia Brasil – Universidade da Integração Internacional da Lusofonia Afro-Brasileira
Prof. Dr. Ferlando Lima Santos – Universidade Federal do Recôncavo da Bahia
Profª Drª Fernanda Miguel de Andrade – Universidade Federal de Pernambuco
Prof. Dr. Fernando Mendes – Instituto Politécnico de Coimbra – Escola Superior de Saúde de Coimbra
Profª Drª Gabriela Vieira do Amaral – Universidade de Vassouras
Prof. Dr. Gianfábio Pimentel Franco – Universidade Federal de Santa Maria
Prof. Dr. Helio Franklin Rodrigues de Almeida – Universidade Federal de Rondônia
Profª Drª Iara Lúcia Tescarollo – Universidade São Francisco
Prof. Dr. Igor Luiz Vieira de Lima Santos – Universidade Federal de Campina Grande
Prof. Dr. Jefferson Thiago Souza – Universidade Estadual do Ceará
Prof. Dr. Jesus Rodrigues Lemos – Universidade Federal do Piauí
Prof. Dr. Jônatas de França Barros – Universidade Federal do Rio Grande do Norte
Prof. Dr. José Max Barbosa de Oliveira Junior – Universidade Federal do Oeste do Pará
Prof. Dr. Luís Paulo Souza e Souza – Universidade Federal do Amazonas
Profª Drª Magnólia de Araújo Campos – Universidade Federal de Campina Grande
Prof. Dr. Marcus Fernando da Silva Praxedes – Universidade Federal do Recôncavo da Bahia
Profª Drª Maria Tatiane Gonçalves Sá – Universidade do Estado do Pará
Profª Drª Mylena Andréa Oliveira Torres – Universidade Ceuma
Profª Drª Natiéli Piovesan – Instituto Federac do Rio Grande do Norte
Prof. Dr. Paulo Inada – Universidade Estadual de Maringá
Prof. Dr. Rafael Henrique Silva – Hospital Universitário da Universidade Federal da Grande Dourados
Profª Drª Regiane Luz Carvalho – Centro Universitário das Faculdades Associadas de Ensino
Profª Drª Renata Mendes de Freitas – Universidade Federal de Juiz de Fora
Profª Drª Vanessa da Fontoura Custódio Monteiro – Universidade do Vale do Sapucaí
Profª Drª Vanessa Lima Gonçalves – Universidade Estadual de Ponta Grossa
Profª Drª Vanessa Bordin Viera – Universidade Federal de Campina Grande
Profª Drª Welma Emidio da Silva – Universidade Federal Rural de Pernambuco

Ciências Exatas e da Terra e Engenharias

Prof. Dr. Adélio Alcino Sampaio Castro Machado – Universidade do Porto
Profª Drª Ana Grasielle Dionísio Corrêa – Universidade Presbiteriana Mackenzie
Prof. Dr. Carlos Eduardo Sanches de Andrade – Universidade Federal de Goiás
Profª Drª Carmen Lúcia Voigt – Universidade Norte do Paraná
Prof. Dr. Cleiseano Emanuel da Silva Paniagua – Instituto Federal de Educação, Ciência e Tecnologia de Goiás
Prof. Dr. Douglas Gonçalves da Silva – Universidade Estadual do Sudoeste da Bahia
Prof. Dr. Eloi Rufato Junior – Universidade Tecnológica Federal do Paraná
Profª Drª Érica de Melo Azevedo – Instituto Federal do Rio de Janeiro

Prof. Dr. Fabrício Menezes Ramos – Instituto Federal do Pará
Profª Dra. Jéssica Verger Nardeli – Universidade Estadual Paulista Júlio de Mesquita Filho
Prof. Dr. Juliano Carlo Rufino de Freitas – Universidade Federal de Campina Grande
Profª Drª Luciana do Nascimento Mendes – Instituto Federal de Educação, Ciência e Tecnologia do Rio Grande do Norte
Prof. Dr. Marcelo Marques – Universidade Estadual de Maringá
Prof. Dr. Marco Aurélio Kistemann Junior – Universidade Federal de Juiz de Fora
Profª Drª Neiva Maria de Almeida – Universidade Federal da Paraíba
Profª Drª Natiéli Piovesan – Instituto Federal do Rio Grande do Norte
Profª Drª Priscila Tessmer Scaglioni – Universidade Federal de Pelotas
Prof. Dr. Sidney Gonçalo de Lima – Universidade Federal do Piauí
Prof. Dr. Takeshy Tachizawa – Faculdade de Campo Limpo Paulista

Linguística, Letras e Artes

Profª Drª Adriana Demite Stephani – Universidade Federal do Tocantins
Profª Drª Angeli Rose do Nascimento – Universidade Federal do Estado do Rio de Janeiro
Profª Drª Carolina Fernandes da Silva Mandaji – Universidade Tecnológica Federal do Paraná
Profª Drª Denise Rocha – Universidade Federal do Ceará
Profª Drª Edna Alencar da Silva Rivera – Instituto Federal de São Paulo
Profª Drª Fernanda Tonelli – Instituto Federal de São Paulo,
Prof. Dr. Fabiano Tadeu Grazioli – Universidade Regional Integrada do Alto Uruguai e das Missões
Prof. Dr. Gilmei Fleck – Universidade Estadual do Oeste do Paraná
Profª Drª Keyla Christina Almeida Portela – Instituto Federal de Educação, Ciência e Tecnologia do Paraná
Profª Drª Miraniilde Oliveira Neves – Instituto de Educação, Ciência e Tecnologia do Pará
Profª Drª Sandra Regina Gardacho Pietrobon – Universidade Estadual do Centro-Oeste
Profª Drª Sheila Marta Carregosa Rocha – Universidade do Estado da Bahia

Conhecimentos pedagógicos e conteúdos disciplinares das ciências exatas e da terra

Diagramação: Maria Alice Pinheiro
Correção: Flávia Roberta Barão
Indexação: Gabriel Motomu Teshima
Revisão: Os autores
Organizador: Francisco Odécio Sales

Dados Internacionais de Catalogação na Publicação (CIP)

C749 Conhecimentos pedagógicos e conteúdos disciplinares das ciências exatas e da terra / Organizador Francisco Odécio Sales. – Ponta Grossa - PR: Atena, 2021.

Formato: PDF

Requisitos de sistema: Adobe Acrobat Reader

Modo de acesso: World Wide Web

Inclui bibliografia

ISBN 978-65-5983-424-2

DOI: <https://doi.org/10.22533/at.ed.242213108>

1. Ciências exatas e da terra - Estudo e ensino. I. Sales, Francisco Odécio (Organizador). II. Título.

CDD 507

Elaborado por Bibliotecária Janaina Ramos – CRB-8/9166

Atena Editora

Ponta Grossa – Paraná – Brasil

Telefone: +55 (42) 3323-5493

www.atenaeditora.com.br

contato@atenaeditora.com.br

DECLARAÇÃO DOS AUTORES

Os autores desta obra: 1. Atestam não possuir qualquer interesse comercial que constitua um conflito de interesses em relação ao artigo científico publicado; 2. Declaram que participaram ativamente da construção dos respectivos manuscritos, preferencialmente na: a) Concepção do estudo, e/ou aquisição de dados, e/ou análise e interpretação de dados; b) Elaboração do artigo ou revisão com vistas a tornar o material intelectualmente relevante; c) Aprovação final do manuscrito para submissão.; 3. Certificam que os artigos científicos publicados estão completamente isentos de dados e/ou resultados fraudulentos; 4. Confirmam a citação e a referência correta de todos os dados e de interpretações de dados de outras pesquisas; 5. Reconhecem terem informado todas as fontes de financiamento recebidas para a consecução da pesquisa; 6. Autorizam a edição da obra, que incluem os registros de ficha catalográfica, ISBN, DOI e demais indexadores, projeto visual e criação de capa, diagramação de miolo, assim como lançamento e divulgação da mesma conforme critérios da Atena Editora.

DECLARAÇÃO DA EDITORA

A Atena Editora declara, para os devidos fins de direito, que: 1. A presente publicação constitui apenas transferência temporária dos direitos autorais, direito sobre a publicação, inclusive não constitui responsabilidade solidária na criação dos manuscritos publicados, nos termos previstos na Lei sobre direitos autorais (Lei 9610/98), no art. 184 do Código penal e no art. 927 do Código Civil; 2. Autoriza e incentiva os autores a assinarem contratos com repositórios institucionais, com fins exclusivos de divulgação da obra, desde que com o devido reconhecimento de autoria e edição e sem qualquer finalidade comercial; 3. Todos os e-book são *open access*, desta forma não os comercializa em seu site, sites parceiros, plataformas de *e-commerce*, ou qualquer outro meio virtual ou físico, portanto, está isenta de repasses de direitos autorais aos autores; 4. Todos os membros do conselho editorial são doutores e vinculados a instituições de ensino superior públicas, conforme recomendação da CAPES para obtenção do Qualis livro; 5. Não cede, comercializa ou autoriza a utilização dos nomes e e-mails dos autores, bem como nenhum outro dado dos mesmos, para qualquer finalidade que não o escopo da divulgação desta obra.

APRESENTAÇÃO

A obra “Conhecimentos pedagógicos e conteúdos disciplinares das ciências exatas e da terra aborda uma série de livros de publicação da Atena Editora, em seu I volume, apresenta, em seus 26 capítulos, discussões de diversas abordagens acerca do ensino e educação. As Ciências Exatas e da Terra englobam, atualmente, alguns dos campos mais promissores em termos de pesquisas atuais. Estas ciências estudam as diversas relações existentes da Astronomia/Física; Biodiversidade; Ciências Biológicas; Ciência da Computação; Engenharias; Geociências; Matemática/ Probabilidade e Estatística e Química. O conhecimento das mais diversas áreas possibilita o desenvolvimento das habilidades capazes de induzir mudanças de atitudes, resultando na construção de uma nova visão das relações do ser humano com o seu meio, e, portanto, gerando uma crescente demanda por profissionais atuantes nessas áreas. A ideia moderna das Ciências Exatas e da Terra refere-se a um processo de avanço tecnológico, formulada no sentido positivo e natural, temporalmente progressivo e acumulativo, segue certas regras, etapas específicas e contínuas, de suposto caráter universal. Como se tem visto, a ideia não é só o termo descritivo de um processo e sim um artefato mensurador e normalizador de pesquisas. Neste sentido, este volume é dedicado aos trabalhos relacionados a ensino e aprendizagem. A importância dos estudos dessa vertente, é notada no cerne da produção do conhecimento, tendo em vista o volume de artigos publicados. Nota-se também uma preocupação dos profissionais de áreas afins em contribuir para o desenvolvimento e disseminação do conhecimento. Os organizadores da Atena Editora, agradecem especialmente os autores dos diversos capítulos apresentados, parabenizam a dedicação e esforço de cada um, os quais viabilizaram a construção dessa obra no viés da temática apresentada. Por fim, desejamos que esta obra, fruto do esforço de muitos, seja seminal para todos que vierem a utilizá-la.

Francisco Odécio Sales

SUMÁRIO

CAPÍTULO 1..... 1

A IMPORTÂNCIA DOS VEÍCULOS AÉREOS NÃO TRIPULADOS (VANT) EM TRABALHOS DE CAMPO E NOS MAPEAMENTOS TEMÁTICOS DE ANÁLISE AMBIENTAL

Victor Hugo Holanda Oliveira

 <https://doi.org/10.22533/at.ed.2422131081>

CAPÍTULO 2..... 12

A HISTÓRIA DA ESTRADA DE FERRO DE ILHÉUS E A TERMODINÂMICA: CONTRIBUIÇÕES AO PROCESSO DE ENSINO E APRENDIZAGEM DE FÍSICA NOS ANOS FINAIS DO ENSINO FUNDAMENTAL

Thais Barbosa dos Santos Moura

Adriano Marcus Stuchi

 <https://doi.org/10.22533/at.ed.2422131082>

CAPÍTULO 3..... 32

AMBIENTE COLOABORATIVO PARA APRENDIZAGEM CONTEXTUALIZADA DE PROGRAMAÇÃO

Maísa Soares dos Santos Lopes

Rodrigo Silva Lima

João Vitor Oliveira Ferraz Silva

Helber Henrique Lopes Marinho

Alzira Ferreira da Silva

Roque Mendes Prado Trindade

Antônio Cezar de Castro Lima

 <https://doi.org/10.22533/at.ed.2422131083>

CAPÍTULO 4..... 47

ANÁLISE DOS PROCESSOS GEOMORFOLÓGICOS COMO SUBSÍDIO AO ORDENAMENTO TERRITORIAL

Karla Nadal

Ronaldo Ferreira Maganhotto

 <https://doi.org/10.22533/at.ed.2422131084>

CAPÍTULO 5..... 60

ANÁLISE TEMPORAL DO ÍNDICE DE VEGETAÇÃO POR DIFERENÇA NORMALIZADA (NDVI) NA REGIÃO NORTE FLUMINENSE

José Carlos Mendonça

Thiago Pontes da Silva Peixoto

Claudio Martins de Almeida

Lorenzo Montovaneli Lazarini

 <https://doi.org/10.22533/at.ed.2422131085>

CAPÍTULO 6..... 74

ANÁLISIS TOPOGRÁFICO Y MORFOMÉTRICO HIDROLÓGICAMENTE CONSISTENTE PARA LA DELIMITACIÓN DE LA CUENCA ILO-MOQUEGUA

Osmar Cuentas Toledo

Alberto Bacilio Quispe Cohaila

Aloísio Machado da Silva Filho

 <https://doi.org/10.22533/at.ed.2422131086>

CAPÍTULO 7..... 86

APPINFOCOVID: APLICATIVO MÓVEL PARA DISPONIBILIZAR INFORMAÇÕES SOBRE A COVID-19

Helder Guimarães Aragão

 <https://doi.org/10.22533/at.ed.2422131087>

CAPÍTULO 8..... 92

CONDIÇÕES SOCIAIS DE SAÚDE, SANEAMENTO E QUALIDADE DA ÁGUA SUBTERRÂNEA DE MUNICÍPIOS DO OESTE DA BAHIA (BR)

Flávio Souza Batista

Manoel Jerônimo Moreira Cruz

Manuel Vitor Portugal Gonçalves

Antônio Bomfim da Silva Ramos Junior

Rodrigo Alves Santos

Cristina Maria Macêdo de Alencar

Débora Carol Luz da Porciúncula

José Jackson de Souza Andrade

Ana Cláudia Lins Rodrigues

 <https://doi.org/10.22533/at.ed.2422131088>

CAPÍTULO 9..... 111

CONSTRUINDO UM CANHÃO ELETROMAGNÉTICO DE BAIXO CUSTO

Carolina Rizziolli Barbosa

João Paulo da Silva Alves

 <https://doi.org/10.22533/at.ed.2422131089>

CAPÍTULO 10..... 117

DETERMINAÇÃO DOS PARÂMETROS CINÉTICOS E TERMODINÂMICOS DA REAÇÃO DE OXIDAÇÃO DO BIODIESEL COMERCIAL SOB EFEITO DE EXTRATO DE ALECRIM (*Rosmarinus Officinalis* L.)

José Gonçalves Filho

Hágata Cremasco Silva

Ana Carolina Gomes Mantovani

Letícia Thaís Chendynski

Karina Benassi Angilelli

Dionisio Borsato

 <https://doi.org/10.22533/at.ed.24221310810>

CAPÍTULO 11	129
ENSINO POR EXPERIMENTAÇÃO-UMA PROPOSTA PARA O ESTUDO LEI DE LAMBERT BEER	
Pedro José Sanches Filho Alex Mercio Mendez Larrosa	
 https://doi.org/10.22533/at.ed.24221310811	
CAPÍTULO 12	144
FEIÇÕES MAGMÁTICAS NA PORÇÃO SUL DA BACIA DE CAMPOS E SUA RELAÇÃO COM O SAL	
Elisabeth de Fátima Strobino Natasha Santos Gomes Stanton	
 https://doi.org/10.22533/at.ed.24221310812	
CAPÍTULO 13	156
GEOPROCESSAMENTO DAS VIAS DE VARRIÇÃO DE REGIÕES DE UMA CIDADE USANDO A FERRAMENTA QGIS	
Jonatas Fontele Dourado Antônio Honorato Moreira Guedes Elias Cícero Moreira Guedes Marcos José Negreiros Gomes	
 https://doi.org/10.22533/at.ed.24221310813	
CAPÍTULO 14	161
INVESTIGANDO FATORES PRIMOS COM TRINCAS PITAGÓRICAS	
Alessandro Firmiano de Jesus João Paulo Martins dos Santos Juan López Linares	
 https://doi.org/10.22533/at.ed.24221310814	
CAPÍTULO 15	176
MODELAGEM DE VAZAMENTOS MARINHOS DE ÓLEO E SUSCETIBILIDADE EM ÁREAS COSTEIRAS E ESTUARINAS	
Caroline Barbosa Monteiro Phelype Haron Oleinik	
 https://doi.org/10.22533/at.ed.24221310815	
CAPÍTULO 16	190
MODELAGEM MATEMÁTICA DA MASSA DE BHA E DE BHT EM BIODIESEL POR REDES PERCEPTRON DE MÚLTIPLAS CAMADAS	
Felipe Yassuo Savada Hágata Cremasco Silva Ana Carolina Gomes Mantovani Letícia Thaís Chendynski Karina Benassi Angilelli Dionisio Borsato	
 https://doi.org/10.22533/at.ed.24221310816	

CAPÍTULO 17	202
O ENSINO DE EXPRESSÕES ALGÉBRICAS ATRAVÉS DA RECEITA DE BRIGADEIRO Jamile Vieira Goi  https://doi.org/10.22533/at.ed.24221310817	
CAPÍTULO 18	207
ONDAS ELETROMAGNÉTICAS NOS LIVROS DIDÁTICOS Leonardo Deosti Ana Suellen Gomes da Silva Hercília Alves Pereira de Carvalho  https://doi.org/10.22533/at.ed.24221310818	
CAPÍTULO 19	220
PROPOSIÇÃO DE MODELOS DE REDUÇÃO DE SONDAGENS BATIMÉTRICAS PARA LEVANTAMENTOS HIDROGRÁFICOS EM RIOS E RESERVATÓRIOS Felipe Catão Mesquita Santos Victória Gibrim Teixeira Mayke Nogueira de Miranda Laura Coelho de Andrade Ítalo Oliveira Ferreira  https://doi.org/10.22533/at.ed.24221310819	
CAPÍTULO 20	236
PRÁTICAS PEDAGÓGICAS APLICADAS A APRENDIZAGEM DE TRABALHOS COM PRESSÕES ANORMAIS Valmir Schork Claudinei Aparecido Pirola  https://doi.org/10.22533/at.ed.24221310820	
CAPÍTULO 21	241
RISK ASSESSMENT FOR EXISTING MINE TAILING STORAGE FACILITIES IN BRAZIL Rafaela Baldi Fernandes Mônica Novell Morell Siefko Slob  https://doi.org/10.22533/at.ed.24221310821	
CAPÍTULO 22	264
SELEÇÃO DE CRITÉRIOS PARA A DETERMINAÇÃO DO NÍVEL DE SIGNIFICÂNCIA EM EIA/RIMA DE ATERROS SANITÁRIOS PELO MÉTODO AHP Renan Costa da Silva Gerson Araujo de Medeiros  https://doi.org/10.22533/at.ed.24221310822	
CAPÍTULO 23	275
SUGESTÕES DE SENSORES DE BAIXO CUSTO PARA ENSINO DE FÍSICA Rodrigo Marques de Oliveira	

Rodrigo Coelho Ramos

Douglas Adolfo Silva

 <https://doi.org/10.22533/at.ed.24221310823>

CAPÍTULO 24.....283

UMA PROSPECÇÃO ANALÍTICA DO POTENCIAL DE TROCADORES DE CALOR SOLO-AR EM PELOTAS

Eduardo de Sá Bueno Nóbrega

Ana Maria Bersch Domingues

Ruth da Silva Brum

Jairo Valões de Alencar Ramalho

Régis Sperotto de Quadros

 <https://doi.org/10.22533/at.ed.24221310824>

CAPÍTULO 25.....294

USO DO *SMARTPHONE* COMO RECURSO DIDÁTICO NO ENSINO EXPERIMENTAL DE FÍSICA

Janaina Zavilenski de Oliveira

Renato Ribeiro Guimarães

Maurício Antonio Custódio de Melo

Luciano Gonsalves Costa

Perseu Ângelo Santoro

 <https://doi.org/10.22533/at.ed.24221310825>

CAPÍTULO 26.....303

UTILIZAÇÃO DE AERONAVE REMOTAMENTE PILOTADA (RPA) PARA GESTÃO TERRITORIAL E AMBIENTAL DA TERRA INDÍGENA PIRAÍ, MUNICÍPIO DE ARAQUARI/SC: ESTRATÉGIAS PARA IMPLEMENTAÇÃO DE PROJETO DE PISCICULTURA

Évelin Moreira Gonçalves

Ângelo Martins Fraga

Laila Freitas Oliveira de Assis

Amanda Elias Alves

Ana Carolina Schmitz da Silva

Felipe Mathia Corrêa

 <https://doi.org/10.22533/at.ed.24221310826>

SOBRE O ORGANIZADOR.....315

ÍNDICE REMISSIVO.....316

RISK ASSESSMENT FOR EXISTING MINE TAILING STORAGE FACILITIES IN BRAZIL

Data de aceite: 20/08/2021

Rafaela Baldi Fernandes

Ph.D. Departamento de Engenharia Civil,
Universidade do Estado do Rio de Janeiro. Rio
de Janeiro, RJ, Brazil

Mònica Novell Morell

BSc. Department of Geoscience and
Engineering, Delft University of Technology (TU
Delft). Delft, The Netherlands

Siefko Slob

PhD. Cohere Consultants. Amersfoort, The
Netherlands

ABSTRACT: This study described is a quick scan of all Tailing Storage Facilities (TSF) in the state of Minas Gerais, Brazil. The objective was to perform analyses, based on gathering information related with TSF's dimensions, purpose, structure and current state. Publicly available data has been used to determine which TSF are most critical. For the most critical dams, a downstream estimation of the drainage path has been performed and the primary and secondary flooding areas due to failure of those dams is estimated. A risk matrix is used to visualise which TSF have the highest risk; additionally, some mitigation and prevention measures are suggested. The report starts with a brief introduction with the present situation in Minas Gerais, as well as a technical description of the project with the results obtained.

KEYWORDS: Dam, Failure, Risk, Management.

RESUMO: Este estudo apresenta um panorama sobre as barragens de rejeito no estado de Minas Gerais, Brasil. O objetivo consiste em analisar estas estruturas baseando-se em informações referentes à dimensão, propósito, tipo de estrutura e estado atual, tendo sido utilizados dados públicos para determinar quais barragens eram mais críticas. Para as barragens mais críticas, elaborou-se uma estimativa da mancha de inundação nas áreas de jusante, primárias e secundárias, decorrente do estudo de ruptura. A matriz de risco foi utilizada para visualizar quais barragens apresentavam maior risco e, adicionalmente, foram sugeridas medidas de mitigação e prevenção de danos. O documento apresenta uma breve introdução da situação atual das barragens em Minas Gerais, além de uma descrição técnica do projeto e dos resultados obtidos.

PALAVRAS - CHAVE: Barragem, Rupturas, Risco, Gerenciamento.

1 | INTRODUCTION

In Brumadinho, on January 25th, 2019, a mine tailing storage facility, dam B-I, from the Vale S.A. mining company failed, which caused 250 casualties and more than 100 people were missing. Nevertheless, it was not the first time that an incident like this one took place; in 2015 near the town of Mariana, the Fundão TSF also failed. The owner of this TSF was the company SAMARCO, a joint venture between Vale S.A. and BHP Billiton.

Cameras were placed around B-I for

monitoring purposes, so there are videos of the failure in real time. Those videos clearly show a slope failure starting from the crest and extending to an area just above the starter dam. The crest of the dam dropped and the area around the toe region bulged outwards before the surface of the dam broke apart. The total collapse happened in less than 10 seconds with $9.7 \times 10^6 \text{ m}^3$ of mudflow that flowed downstream at a high speed (Robertson et al., 2019).

When a dam fails, loss of life, environmental, human and economic damage are direct consequences of such an event, which depend on the magnitude of the mudflow and its velocity. Therefore, early warning is essential for saving lives in areas at risk for mudflows.

2 | TYPES OF TAILINGS DAMS

Tailing dams are embankments made of waste material, product of many years of mining activities. These occupy large areas and hold large volumes of fine-grained tailing material. There are three different types of construction methods for tailing dams: upstream, downstream and centerline (see Figure 1).

- **Upstream:** the first dike is constructed at ground level in a valley, hence the valley walls become the support for the tailing sides. The mining waste is hydraulically placed behind the dike and once all the volume is filled up, a second dike is constructed on top of the previous one. Part of the new dike will be placed on top of the first one and the remaining part on top of the waste, moving the crest further upstream. This procedure can be done multiple times, creating an upstream dam with 3 or more different sub-dams, which are laying on top of each other. The height and volume of the structure will drastically increase every time, making it very unstable, since part of the dam is resting in weak material from mining activities, probably saturated and prone to liquefaction (Dutch Risk Reduction Team, 2019).
- **Downstream:** the first dike is also constructed at ground level in a valley. Once the volume behind the dam is as its maximum, the next dam is placed on top of the previous one, but the extra support needed is placed in front of the starter dike, thus raising the crest further downstream. This method requires more material and available space for the upcoming new dams.
- **Centerline:** like both other methods, the starter dam is at ground level. When subsequent raising is required, material is placed on the tailing and the existing embankment. Thus, the crest will raise vertically.

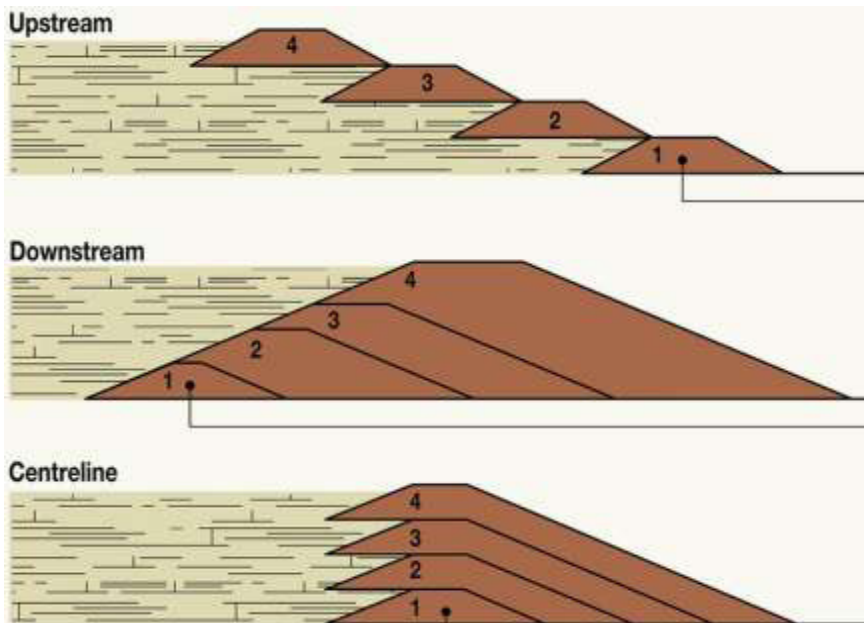


Figure 1. Types of tailing dams. (Source: www.grida.no)

From the three construction methods, tailing dams constructed by the conventional upstream method are the most unstable. Their shear strength and pore pressure conditions are difficult to characterize. If the groundwater pressure increases, seepage or liquefaction might happen, thus the dam could collapse, allowing the material to flow out, uncontrollably (Martin, 1999).

Now, there are 430 tailing dams in the state of Minas Gerais, from which 50 were designed and constructed in the same way as dam B-I. 30 of them are still operational and the other 20 are filled up with their maximum capacity.

2.1 Classification organizations

One of the main issues with those dams is that it is unclear how they were designed, constructed, and operated. In some cases, the dam raises higher than what had been originally planned. Additionally, proper documentation related with the design and construction methods is lacking (Dutch Risk Reduction Team, 2019).

In order to classify all the dams in Brazil, there are several classification systems: *FEAM* (Fundação Estadual do Meio Ambiente), *ANM* (Agência Nacional de Mineração) and *ANA* (Agência Nacional de Águas), like described in Fernandes (2020). The three organizations classify all dams in Minas Gerais according to several properties related with the structure of the dam itself and also the risk associated. For all three organizations, there are properties which are the same within all three databases, such as: TSF name, company owner, coordinates, volume and height. Nonetheless, for each system there are additional

features that give extra information on those dams.

2.1.1 FEAM: Fundação Estadual do Meio Ambiente

Fundação Estadual do Meio Ambiente published a database with 700 entries. In addition to the previous characteristics, information related with the risk associated is given.

The hazard level is divided in three different categories (I, II, III), which depend on the combination between only two different values of V_c . Each attribute has specific value of V_c according to its magnitude (FEAM, Sistema Estadual de Meio Ambiente e Recursos Hídricos, 2018). The characteristics considered and the given values for V_c are displayed in Table 1:

Height [m]	Volume [m ³]	Cities Nearby	Environmental Impact	Structures Nearby
H<15 $V_c = 0$	$V_r < 500.000$ $V_c = 0$	None $V_c = 0$	Low $V_c = 0$	None $V_c = 0$
15<H<30 $V_c = 1$	$500.000 < V_r < 5 \text{ m}$ $V_c = 1$	Barely $V_c = 2$	Medium $V_c = 1$	Some $V_c = 1$
H>30 $V_c = 2$	$V_r > 5 \text{ m}$ $V_c = 2$	Some $V_c = 3$	High $V_c = 3$	Large $V_c = 2$
-	-	Large $V_c = 4$	-	-

Table 1. Assessment criteria for environmental impact for a TSF. (Source: FEAM (2018)).

The three different categories are defined according to the sum of two values of V_c :

- Low impact in the area. Class I: $V_c \leq 2$;
- Medium impact in the area. Class II: $2 < V_c \leq 5$; and
- High impact in the area. Class III: $V_c > 5$,

On February 25, 2021 a new resolution was published, regulating new devices for classifying dams and auditors. However, data with this new database have not yet been released.

2.1.2 ANM: Agência Nacional de Mineração

Agência Nacional de Mineração also published a TSF database with 850 entries. Apart from the most common properties, there are also some different characteristics (ANM, Agência Nacional de Mineração, 2019).

A. Risk level (CRI): associated risk according to the structural and technical characteristics of the dams. The categories are:

- High
- Medium

- Low

B. Potential damage associated (PDA): degree of damage in the environment in case of failure. It is linked with the volume of the reservoir (V_r in m^3). The categories are:

- Very high ($V_r \geq 50 \cdot 10^6$)
- High ($25 < V_r < 50 \cdot 10^6$)
- Medium ($5 < V_r < 25 \cdot 10^6$)
- Low ($500.000 < V_r < 5 \cdot 10^6$)
- Very low ($V_r \leq 500.000$)

C. Class: product between CRI and PDA. Class A corresponds to the most critical state. The categories can be seen in Table 2:

CRI	PDA		
	High	Medium	Low
High	A	B	C
Medium	B	C	D
Low	B	C	E

Table 2. Different classes according to CRI*PDA. (Source: ANM, 2019).

D. Emergency level: according to a team of experts, the need for a TSF to be improved:

- Level 1: irregularity detected
- Level 2: risk under control
- Level 3: imminent failure

2.1.3 ANA: Agência Nacional de Águas

Agência Nacional de Águas makes an annual database with all the dams (19.388 structures) in Brazil in order to present their current state. Because it is a general database, there are dams which belong to different organisations, such as *IMAC* - Instituto de Meio Ambiente do Acre or *IPAAM* - Instituto de Proteção Ambiental do Amazonas (ANA, Agência Nacional de Águas e Saneamento Básico, 2019).

ANA's database contains most dam structures of the country, but not all of them. From that database, only the TSF that belong to *ANEEL* (Agência Nacional de Energia Elétrica) are added in the final database (905 entries).

3 | RESULTS

3.1 Final database of all mine tailing storage facilities

After analysing all the excel files, there are some discrepancies between the three databases. When looking at the same structure, it is possible that it has the same name in all files, but different coordinates, identification code or information regarding the risk associated.

A unique database that would contain information from all sites was developed from different databases. Therefore, after combining all inputs, merging the information, and making sure that some were not doubled, a final database with 743 entries was obtained. The following table (see Table 3) shows the 10 most critical tailing dams in Minas Gerais. All of them are upstream dams, with a high CRI and PDA and sorted by their height.

The database contains the exact location of each TSF along with other metadata. Since some mine tailing dams were repeated in two or three original databases (*ANM*, *FEAM* or *ANA*), then all the inputs that were duplicated had been merged into a unique entry. The final database is exported into a shapefile, which can be uploaded in QGIS. QGIS allows to view all the TSF locations with for instance Google Satellite as a background image (see Figure 2). The Attribute Table of the shapefile contains all the metadata from the excel file, therefore it is easy to locate one TSF and check its information.

TSF Name	Organization	Elevation of the crest (II) [m asl]	Dam Height [m]	Volume [m ³]
Campo Grande	ANM+FEAM	940	99.3	23 * 10 ⁶
Forquilha I	ANM+FEAM	1175	98.3	13 * 10 ⁶
Barragem de Rejeitos	ANM	972	89	5 * 10 ⁶
Forquilha II	ANM+FEAM	1173	88	23 * 10 ⁶
Sul Superior	ANM+FEAM	923	85	6 * 10 ⁶
Forquilha III	ANM+FEAM	1099	77	19 * 10 ⁶
Doutor	ANM+FEAM	751	77	38 * 10 ⁶
ED Xingu	ANM	965	70	6 * 10 ⁶
Grupo	ANM+FEAM	1140	39	1 * 10 ⁶
Vargem Grande	ANM+FEAM	1282	35	10 * 10 ⁶

TSF Name	CRI	PDA	Class	Class	Emergency Level
Campo Grande	High	High	A	III	Level 1
Forquilha I	High	High	A	III	Level 3
Barragem de Rejeitos	High	High	A		Level 2
Forquilha II	High	High	A	III	Level 2
Sul Superior	High	High	A	III	Level 3
Forquilha III	High	High	A	III	Level 3
Doutor	High	High	A	III	Level 2
ED Xingu	High	High	A		Level 1
Grupo	High	High	A	III	Level 2
Vargem Grande	High	High	A	III	Level 1

Table 3. The 10 most unstable tailing dam facilities. (Source: *ANM* and *FEAM*).

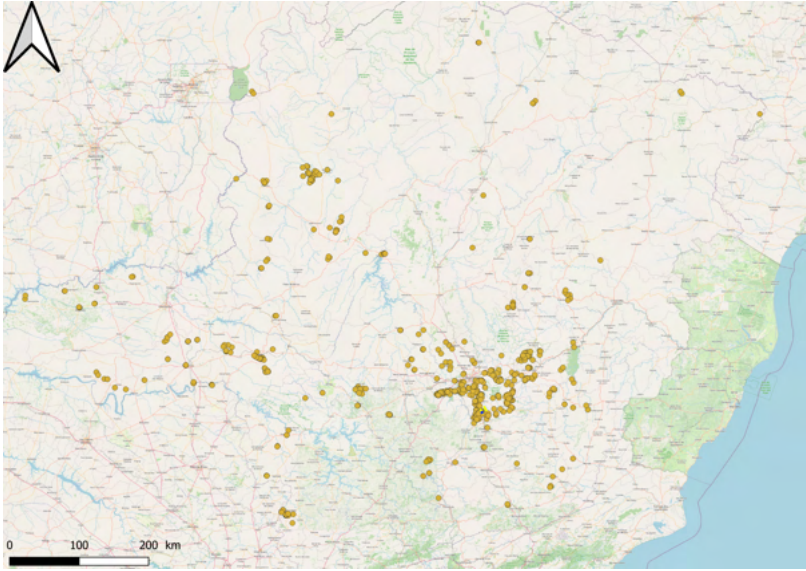


Figure 2. TSF locations in Minas Gerais, visualization with QGIS.

3.2 Risk assessment: primary Impact Zone

To assess the impact of dam failure, the flooding area has been estimated according to the geometry and volume of the reservoir and the downstream area. According to Federico and Cesali (2015), there are several empirical relationships that allow a preliminary approximation of run-out distances. In this project, the formula suggested by Corominas (1996) is used to determine the primary impact zone in case of dam breach.

The equation estimates the angle of reach (α), which is the ratio of the elevation difference between the highest point of the granular mass before sliding and the more advanced point of deposit after sliding (H) and the total travelled distance of the waste material (L) (see equation 1).

$$\tan(\alpha) = \frac{H}{L} \quad (1)$$

Corominas (1996) also suggested an empirical expression that links the H/L ratio with the total volume of the mass (V) for all kinds of landslides (translational slides, rockfall, avalanches, debris flows, mudflows). It is noted that the ratio decreases when the total volume increases, thus the larger the volume the larger is the travelled distance (L). The formula proposed is:

$$\frac{H}{L} = 0.973 \cdot V^{-0.105} \quad (2)$$

From the database created, the volume of each reservoir is given, therefore the ratio H/L is known from equation 2. The value obtained can be used to estimate the angle of reach with equation 1.

Additionally, an energy-based approach has been carried out with QGis. Before collapse, the waste volume has a certain potential energy, which after failure becomes partly kinetic and partly potential energy. To estimate the flooding area in case of dam breach, the idea is to create an energy plane that has the same height as the dam at that specific location (respect mean sea level) and the same angle of reach found with equation 1. Then, the energy plane is extended downstream and above the topography, until a certain point where the energy plane will cross the surface.

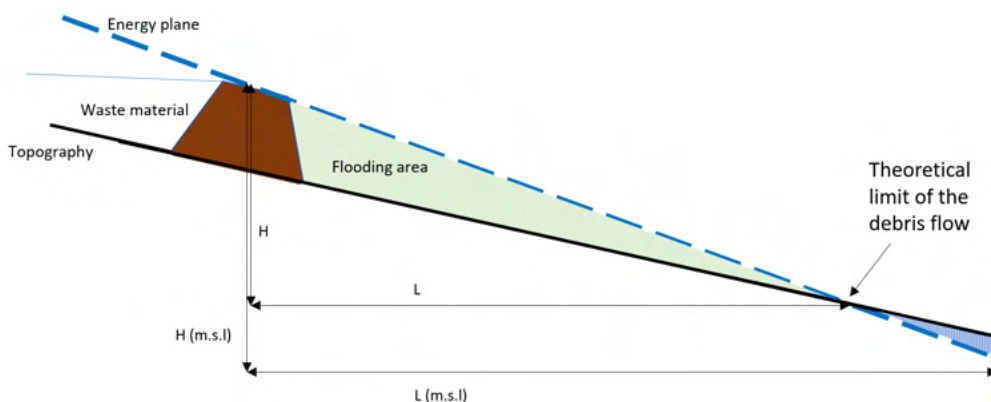


Figure 3. Sketch of the energy plane along with the topography.

As it was mentioned before, the energy plane has a certain slope, which is higher than the topography (Figure 3). This 2D plane is created with a first line that follows the crest width of the dam and a second parallel line located at a certain distance (L) from the TSF. The angle of reach found determines the slope of the energy plane, and with the H value, L can be calculated. Then, the second line will be moved in parallel at a specific distance L from the crest dam; elevation value assigned at that line will be the one of the drainage paths at that exact cutting point (line-drainage path). Once both lines are located, lineal interpolation between these two allows to fill in all the missing elevation values and have the final energy plane. The interpolated map needs to have the same cell size and dimensions as the Digital Terrain Model (*DTM*) of the area.

To determine the flooding area, it is possible to subtract the *DTM* from the interpolated map. When the energy plane is above the topography, all the area in between will have positive values, which corresponds to the flooding area (green area in Figure 3). When the energy plane crosses the topography, that theoretical limit corresponds to the area at risk for flooding by debris flow.

To demonstrate the aforementioned method, equation 2, 1 and the energy model have been validated with the characteristics of the dam B-I failure.

3.2.1 Validation of the formula with dam B-I

Because there is enough public data about the disaster of dam B-I, it is possible to back calculate the flooding area and the angle of reach. The volume of the first flood wave is known ($V = 9.7 * 10^6 \text{ m}^3$), so the angle of reach (α) can be measured following equation 2 and then equation 1.

To verify the previous result, the energy plane is created with QGis to check whether L (yellow line from Figure 5) from the equations is consistent with the extent of the flooding area from Ghahramani et al. (2020) studies. The elevation of the crest was 920 m (m.s.l) and the dam's height 80 m. According to Ghahramani et al. (2020), the furthest point of the deposit after failure was at 5.5 km of the TSF (following a straight line) and at 740 m (m.s.l) (see Figure 4 for a sketch of the situation). The energy plane in QGis can be seen in the following picture. It is a raster layer created with Interpolation TIN tool between the two lines (see Figure 5).

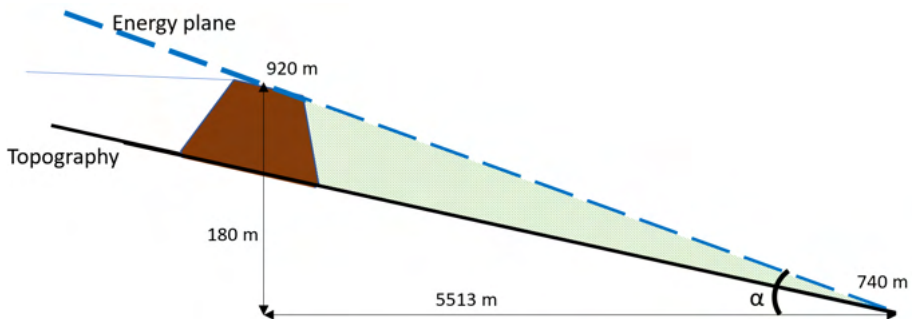


Figure 4. Sketch of the energy plane according to the dam B-I disaster.

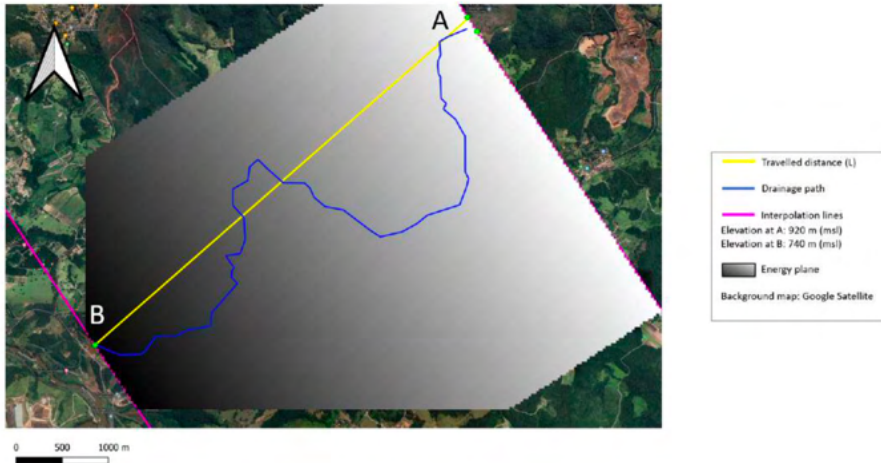


Figure 5. Energy plane created from the two purple lines.

The resulting flooding area is showed in red in Figure 6 and the blue line represents the drainage path that the waste material followed after failure. The primary impact zone after failure, according to Ghahramani et al. (2020), is showed in red in Figure 7, which has the same extent as the one found with the energy plane with QGis.

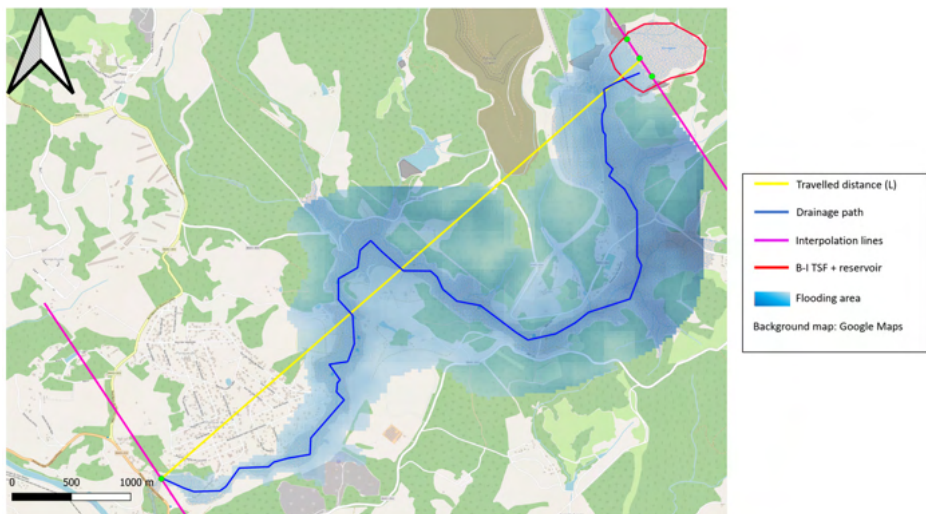


Figure 6. Flooding area for the dam B-I disaster. (QGis approach).

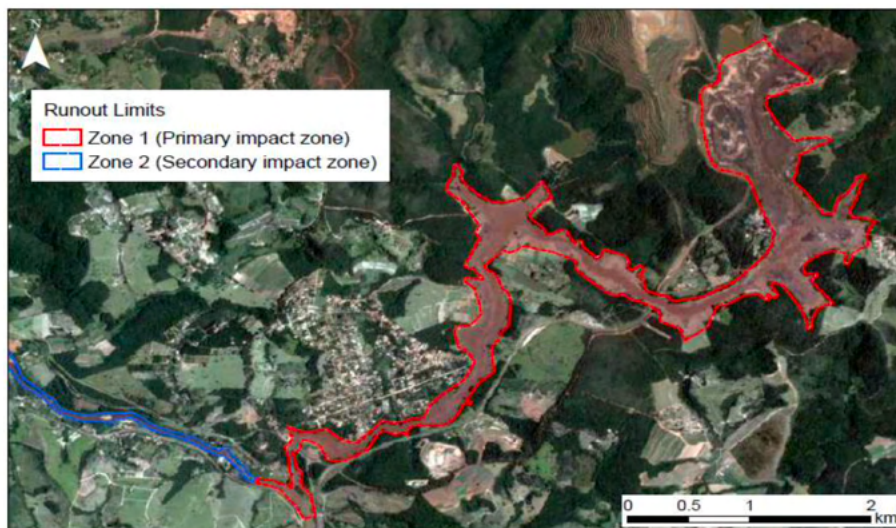


Figure 7. Primary impact zone according to Ghahramani et al. (2020).

Comparing Figure 6 and 7, the flooding area obtained with QGIS (red area in Figure 6) is wider along the drainage path than the primary impact zone according to Ghahramani et al. (2020). QGIS acts as a conservative method, as the flooding area near the dam is over estimated. In the lower range, QGIS underestimates that area as it is less than reality. Further studies could be carried out to narrow down the affected area in the entire zone.

Therefore, it can be concluded that the aforementioned method, first use the empirical relationship presented by Corominas (1996) to calculate the angle of reach and secondly, create energy plane to subtract from it the topography; it is an accurate approach to determine the deposit in case of failure of mine tailing dams, and the consequent impact of the first wave.

3.2.2 Campo Grande Dam

According to Table 3, Campo Grande Dam is the highest TSF and it has been analysed to visually represent the potentially hazardous area in case of a dam breach. Campo Grande is an upstream dam which belongs to the Mariana complex and Alegria mine, although its lifespan ended in 2017. From the ANM database it can be seen that Campo Grande contains 23 million m³ of waste material, it has a height of 99.3 m and it is situated at an elevation (crest level) of 940 m with respect to mean sea level.

First of all, the angle of reach is $\alpha = 9.3^\circ$, it is calculated according to the given volume of Table 3, equation 2 and equation 1. H is the elevation of the crest respect to mean sea level ($H=940$ m). Thereafter, with α and H , the horizontal extension of the energy plane can be determined (see Figure 3 for a sketch). This measured distance, $L = 5727$

m, is projected in the DTM of the area along a straight line that starts in the TSF's crest (yellow line in Figure 8). The line that follows the crest width is copied and moved in parallel downstream at a certain distance L , and its elevation is the same as the drainage path at that cutting point. Interpolation between those two lines is done and finally, subtraction of the DTM from the interpolated map. The resulting red area corresponds to the primary impact zone after dam failure (see Figure 8).

From Figure 8, the red area corresponds to the flooding area in case of dam breach, since the energy plane is above the topography. Furthermore, it is possible to have additional red zones because there are other valleys in the area, but those red zones are not representative for the Campo Grande failure.

In accordance with the procedure explained before, one might expect that the flooding area would be extended until the second line. However, it is important to consider the topography of the area. The drainage path has been converted into a layer of points and for each point, the elevation is assigned. It can be proved that the topography is not always decreasing along the path, therefore the primary flooding area is reduced. Although, it will continue flowing downstream, since it follows the Piracicaba river course.

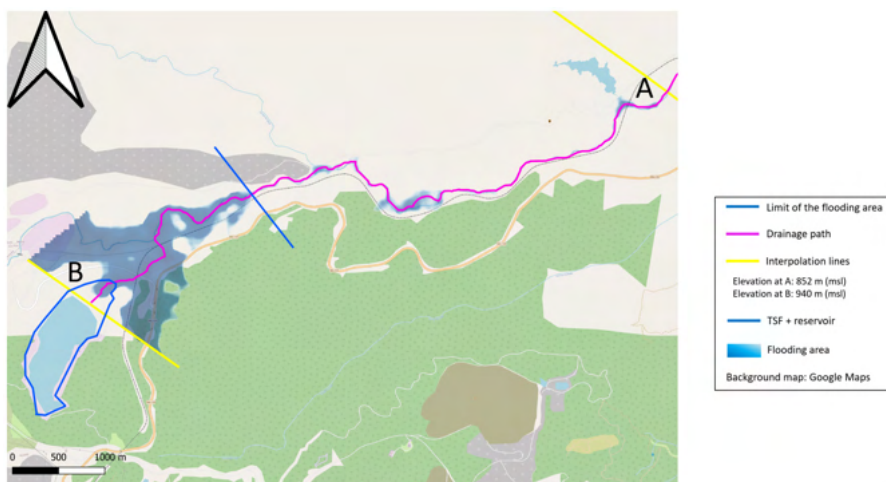


Figure 8. Flooding area in case of Campo Grande failure.

3.2.3 Others mine tailing storage facilities

The others TSF's from Table 3 are also analysed. The procedure is the same as the one described in section 3.2.2. The results can be seen in the following table (see Table 4) and the resulting maps in the Appendix.

According to the results obtained, it is possible to have a general overview of the estimation could be used as a first approach to delimit the risk area in case of dam failure. To complete the risk assessment, the following section introduces which mine tailing

dams involve higher risks and their level of exposure due to collapse along with mitigation measures.

Name	Elevation of the crest [m a.s.l.]	Elevation Downstream [m a.s.l.]	Dam Height [m]	Volume [m ³]	H/L ratio
Campo Grande	940	852	99.3	23 * 10 ⁶	0.1641
Forquilha I	1175	945	98.3	13 * 10 ⁶	0.1746
Barragem de Rejeitos	972	801	89	5 * 10 ⁶	0.1916
Forquilha II	1173	942	88	23 * 10 ⁶	0.1643
Sul Superior	923	756	85	6 * 10 ⁶	0.1889
Forquilha III	1099	903	77	19 * 10 ⁶	0.1670
Doutor	751	711	77	38 * 10 ⁶	0.1558
ED Xingu	965	871	70	6 * 10 ⁶	0.1884
Grupo	1140	891	39	1 * 10 ⁶	0.2228
Vargem Grande	1282	791	35	10 * 10 ⁶	0.1801

Name	Reaches Angle [°]	L' [km]	Drainage path length [km]
Campo Grande	9.3	5.7	2.8
Forquilha I	9.9	6.7	9.4
Barragem de Rejeitos	10.9	5.1	8.7
Forquilha II	9.3	7.1	9.9
Sul Superior	10.7	4.9	11.3
Forquilha III	9.5	6.6	12.1
Doutor	8.9	4.8	4.0
ED Xingu	10.7	5.1	5.2
Grupo	12.6	5.1	17.0
Vargem Grande	10.2	7.1	5.9

Table 4. Values obtained for the most 10 unstable TSF.

3.2.4 Risk management plan

From the previous results, a risk matrix is created to estimate the level of risk of each TSF by considering the category of Hazard, which is associated with the distance of the flooding area along the drainage path against the category of Exposure, which quantifies the number of man-made infrastructures encountered along the drainage path.

The exposure axis is made according to the number of structures along the drainage path and a vulnerability number ranging from 1 to 5 that has been assigned to different possible constructions (see Table 5). For each TSF analysis, every single structure affected by the flooding area is considered and the average value of vulnerability is calculated respect 5. The hazard axis is the ratio of the drainage path extension by 5. Thus, a 5x5 risk matrix can be created.

Both axes go from 1 to 5, being 1 the lowest threat. Once plotted the calculated values of hazard vs. exposure, it can be seen the position of each tailing dam and its risk involved, according to the background colour of the chart (see Figure 9).

Structure	Vulnerability
Cities	5
Roads	3
Train tracks	3
Mining complex	3
Other TSF	2

Table 5. Risk values assigned for each structure.

When analysing the previous chart, for instance, Grupo dam provides a threat in terms of the length of its drainage path, but since the level of exposure is less than 2, it means that not many man-made structures will be compromised, in this case, only roads and train tracks. Sul Superior and Vargem Grande are the TSF with highest level of exposure, but Sul Superior has a larger drainage path, hence it is located near the moderate-risk zone. In case of failure, both principal flooding areas would impact cities and roads. But, in the case of Sul Superior, it would also affect a mining complex; and Vargem Grande would damage several train tracks.

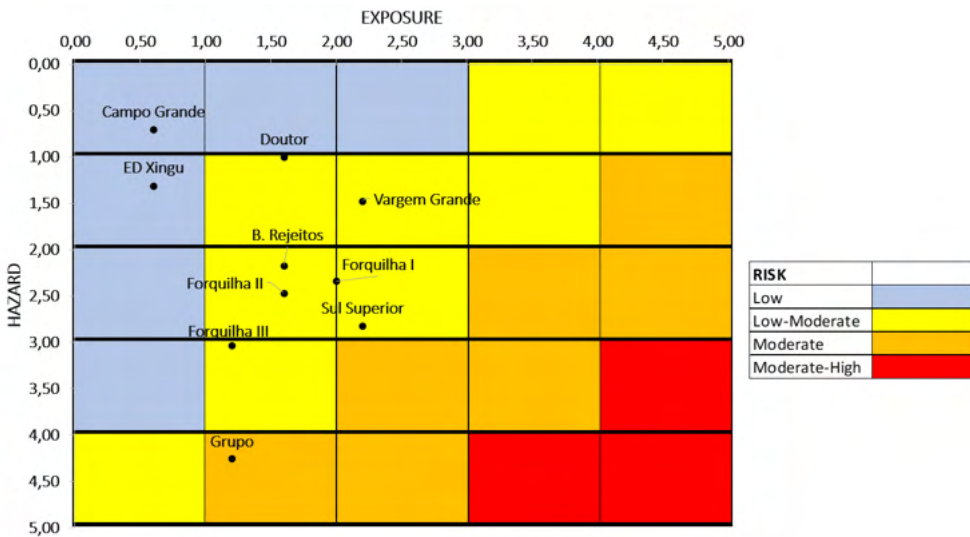


Figure 9. Risk matrix.

Most dams fall in the category of Low-Moderate risk, except Grupo dam, which is in a higher category. Within this level, the number of structures encountered, and the length of the drainage path make the difference. However, none of the dams is within the Moderate-High level; to be in the red area, the length of the drainage path should be at least 12 km and pass through more than one city, roads and train tracks.

Although the risk involved depends on several inputs, it is true that possible failure

would imply socio- environmental effects that will persist for a long period of time. A risk reduction campaign would involve defining the present level of risk and try to reduce it to an acceptable value and implement an emergency plan to ensure the safety of the citizens nearby.

There are two different approaches to minimise the risk. On one hand, try to improve the current structure of the dam; on the other hand, damage containment mechanisms for the downstream valley and an emergency response plan for citizens in case of accident.

In order to improve the present conditions of mine tailing dams, a general maintenance of the structure should be carried out, as well as an improved surveillance and monitoring plan. Another option is to excavate wells outside of the danger area, with the aim to lower the water level in the dam and avoid liquefaction or seepage. Now, Vale S.A. is performing a decommissioning process in some upstream dams; the plan is based on imminent closure of those dams and start removing all the waste material in order to recover the previous environment.

The downstream area is at high risk in case of accident, because, unlike water, the mass of tailings is such that it can cause great damage, much greater than that of an equivalent flood of water, demolishing buildings rather than just flowing through them. Thus, approaches to risk reduction for the downstream valley system include the preparation of inundation maps, estimation of the time of arrival of the flood wave at different locations, the duration of inundation, implementation and maintenance of emergency warning procedures and systems (Penman, 2001).

As an example, in the case of the Sul Superior dam, a Rolled-Compacted Concrete (RCC) containment dam is being constructed downstream of it (see Figure 10). This dam has a volume of 175.000 m³ and it is built in lifts of 40 cm (Dutch Risk Reduction Team, 2019).



Figure 10. RCC containment dam below Sul Superior.

3.3 Risk assessment: Secondary Impact Zone

The sections before were focused on the damage evaluation within the area. However, it is also important to consider the final extension and the negative effects that such failure would cause in the long term. Concha Larrauri and Lall (2018) presented a model to estimate the volume released of tailings and the maximum distance travelled by them. Different parameters are needed, such as the total impounded volume (V_T) in m³ and the dam's height (H) in m.

First of all, from the impounded volume it is possible to estimate the total volume of tailings that could be released (V_F). According to Rico et al. (2008), the total volume of tailings due to failure typically ranges from 10 to 35% of the impounded tailings volume. For this section, it is assumed that the volume data from Table 3 is V_T , since not the entire mass retained by the dam will flow out.

The formula suggested by Concha Larrauri and Lall (2018) to calculate V_F is:

$$V_F = 0.332 \cdot V_T^{0.95} \quad (3)$$

Once the volume is known, the variable H_f is introduced to consider the potential energy associated with the previous released volume:

$$H_f = H \cdot \left(\frac{V_F}{V_T}\right) \cdot V_F \quad (4)$$

Finally, the maximum run-out distance (D_{max}) can be calculated:

$$D_{max} = 3.04 \cdot H_f^{0.545} \quad (5)$$

Using the equations, the maximum run-out distance reached by tailing materials along the drainage path is displayed in the following Table 6.

Some of the results obtained regarding the maximum run-out distance (D_{max}) are not consistent with the ones found before (Table 3). For example, in the case of Grupo dam, where the model proposed by Concha Larrauri and Lall (2018) suggests a travelled distance of 7.51 km in total, whereas with the QGis approach the distance measured is 17.0 km, only for the primary impact zone.

Name	Dam Height [m]	Volume [m ³]	Final Volume (V _r) [m ³]
Campo Grande	99.3	23 * 10 ⁶	6.5 * 10 ⁶
Forquilha I	98.3	13 * 10 ⁶	3.7 * 10 ⁶
Barragem de Rejeitos	89	5 * 10 ⁶	1.6 * 10 ⁶
Forquilha II	88	23 * 10 ⁶	6.5 * 10 ⁶
Sul Superior	85	6 * 10 ⁶	1.8 * 10 ⁶
Forquilha III	77	19 * 10 ⁶	5.6 * 10 ⁶
Doutor	77	38 * 10 ⁶	10.4 * 10 ⁶
ED Xingu	70	6 * 10 ⁶	1.9 * 10 ⁶
Grupo	39	1 * 10 ⁶	0.4 * 10 ⁶
Vargem Grande	35	10 * 10 ⁶	2.8 * 10 ⁶

Name	Hr	Runout Distance (D _{max}) [km]
Campo Grande	183.8	52.1
Forquilha I	107.2	38.8
Barragem de Rejeitos	43.6	23.8
Forquilha II	161.6	48.6
Sul Superior	47.1	24.8
Forquilha III	122.8	41.8
Doutor	222.5	57.8
ED Xingu	39.7	22.6
Grupo	5.3	7.5
Vargem Grande	29.7	19.1

Table 6. Maximum run-out distances for each mine tailing dam.

This deviation can be caused by the different values of volume used, since the QGIS method used the total volume of the reservoir. However, the Concha Larrauri and Lall (2018) method does not consider the topography of the area, thus it could be the case of possible obstacles along the drainage path that would reduce the run-out distance in reality.

3.3.1 Risk management plan

To reduce the impact in response to dam failure, a risk management plan evaluates the effects involved in the entire downstream area affected, which in the long term will be more environmental and social related. Mining industries produce large volumes of waste, which are stored in impoundments behind dams and in case of collapse, all this material would flow out.

Environmental impacts in the downstream area depend on the magnitude and the toxicity of the materials. The ensuing discharge into river systems would affect the water quality, thus the aquatic and human life. Therefore, it would be necessary a study regarding the type of material involved, the usage of water of the polluted river and the impact on the flora and fauna. Spillage of tailings dam in the environment have immediate negative effects in the surroundings. If clean-up operations are not performed, chemical concentrations in the environment will decrease over time, due to aqueous dilution and sedimentation of other materials (Kossoff et al., 2014).

There are some mitigation measures which can be carried out in order to reduce

the impact, but completely erasing the damage would not be possible. A first option is to add chemicals into the polluted soils to reduce the mobility of the contaminants or neutralize its negative effects. Secondly, the construction of barriers to contain the waste material and prevent it from spreading further. Nevertheless, the most common practice is to remove the spillage material from the affected area and store it into another location (Kossoff et al., 2014).

4 | CONCLUSIONS AND RECOMMENDATIONS

Mine tailing dam failures are a serious threat to the downstream environment and human-made structures, because the sudden release of large quantities of tailings into river catchments poses a serious threat to animal and human health. This report presents a simple and effective method to determine the primary flooding area in case of dam failure. It is based on the empirical relationship presented by Corominas (1996), which allows to determine the angle of reach, thus the length of the deposit in the horizontal plane.

The first challenge encountered was the amount of data available, but at the same time the contradictions in it regarding some structures. From the database created, it is possible to identify the TSF based on their risk level, however, it is not possible to derive the (geotechnical) stability or safety factor. This requires a very specific analysis, which falls outside the scope of this study. The first step of the project was to create a general database with all available information from all structures. Now, it is possible to visualise in QGIS the location and the metadata of all TSFs in Minas Gerais.

From the results in Table 4 and according to Corominas' empirical relationship the more volume involved in failure, the smaller is the value of angle of reach. Thus, more volume means that the travelled distance by the waste material will increase, so the energy plane will be less steep. With the angle of reach, the energy plane was created according to elevation values and the initial flooding area obtained. It is important to check the topography of the area, because it is possible that the flooded area is smaller than expected because of irregularities along the drainage path, such as a sudden change in the slope downstream the dam.

The risk matrix created outlines which TSF has the highest risk, which is defined by the factor of hazard in combination with the exposure to the hazard. Therefore, the mine tailing dam Sul Superior is the most vulnerable of all TSF, because of the man-made structures along its drainage path, even though Grupo dam has a more extensive flooded area.

The results provided in this study are a starting point to have a first idea of the areas affected by a debris flow resulting from a dam failure. However, the procedure followed is useful, it is at the same time manual and slow. Some recommendations for further studies would imply using complex flow models to obtain more accurate results and to automatise the procedure to analyse more possible failure dams.

REFERENCES

ANA, Agência Nacional de Águas e Saneamento Básico. (2019). Relatório de Segurança de Barragens. ANM, Agência Nacional de Mineração. (2019). Relatório Anual de Segurança de Barragens de Mineração.

Concha Larrauri, P., & Lall, U. (2018). Tailings dams failures: Updated statistical model for discharge volume and runout. *Environments*, 5 (2), 28.

Corominas, J. (1996). The angle of reach as a mobility index for small and large landslides. *Canadian Geotechnical Journal*, 33 (2), 260–271.

Dutch Risk Reduction Team. (2019). DRR Team Mission Report Minas Gerais state, Brazil.

FEAM, Sistema Estadual de Meio Ambiente e Recursos Hídricos. (2018). Assessoria de Normas e Procedimentos.

Federico, F., & Cesali, C. (2015). An energy-based approach to predict debris flow mobility and analyse empirical relationships. *Canadian Geotechnical Journal*, 52 (12), 2113–2133.

Ghahramani, N., Mitchell, A., Rana, N. M., McDougall, S., Evans, S. G., & Take, W. A. (2020). Tailings-flow runout analysis: Examining the applicability of a semi-physical area–volume relationship using a novel database. *Natural Hazards and Earth System Sciences*, 20 (12), 3425–3438.

Kossoff, D., Dubbin, W., Alfredsson, M., Edwards, S., Macklin, M., & Hudson-Edwards, K. A. (2014). Mine tailings dams: Characteristics, failure, environmental impacts, and remediation. *Applied Geochemistry*, 51, 229–245.

Martin, T. (1999). Characterization of pore pressure conditions in upstream tailings dams. *Tailings and Mine Waste*, 99, 303–313.

Penman, A. (2001). Tailings dams: Risk of dangerous occurrences. *Geoenvironmental Engineering: Geoenvironmental Impact Management: Proceedings of the third conference organized by the British Geotechnical Association and Cardiff School of Engineering, Cardiff University, and held in Edinburgh on 17–19 September 2001*, 150–156.

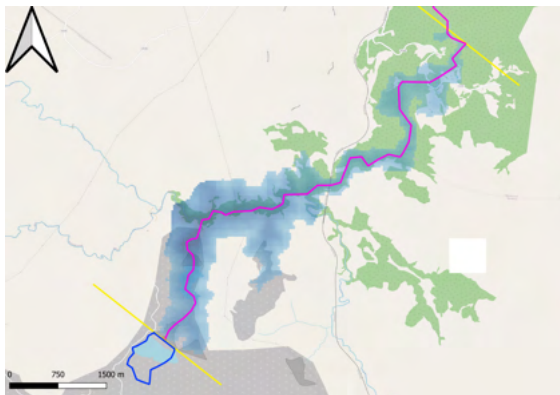
Rico, M., Benito, G., & Diez-Herrero, A. (2008). Floods from tailings dam failures. *Journal of hazardous materials*, 154 (1-3), 79–87.

Robertson, P. K., De Melo, L., Williams, D. J., & Wilson, G. W. (2019). Report of the Expert Panel on the Technical Causes of the Failure of Feijão Dam I.

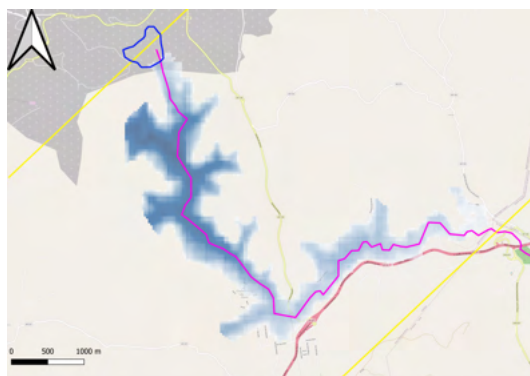
NOTE

This material is part of the studies at Delft University of Technology - Internship at Cohere Consultants, in Amersfoort, by Mònica Novell Morell.

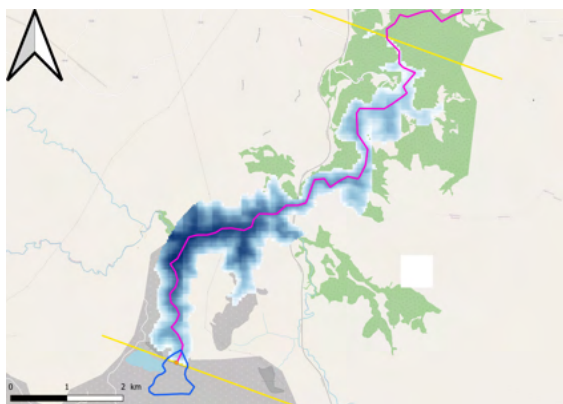
APPENDIX



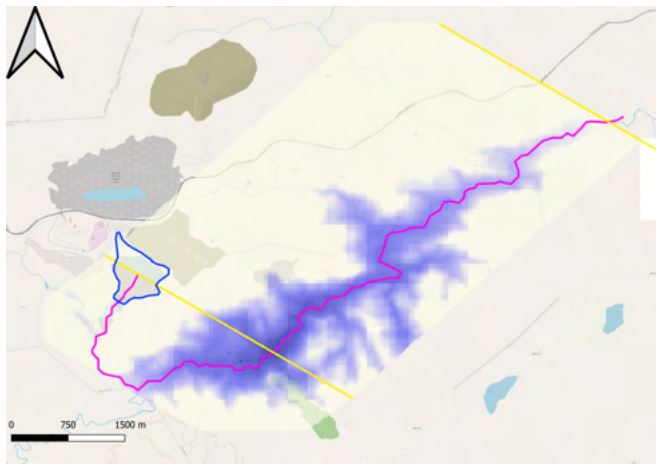
1. FORQUILHA I



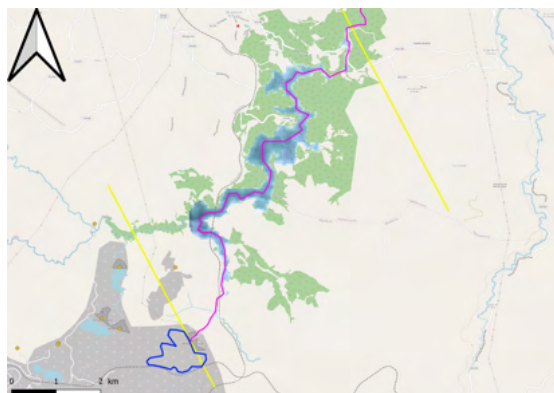
2. BARRAGEM DE REJEITOS



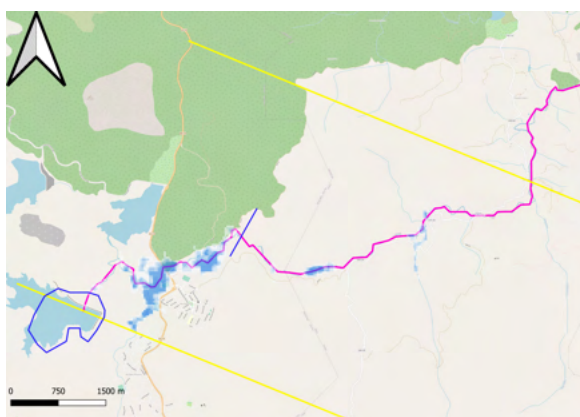
3. FORQUILHA II



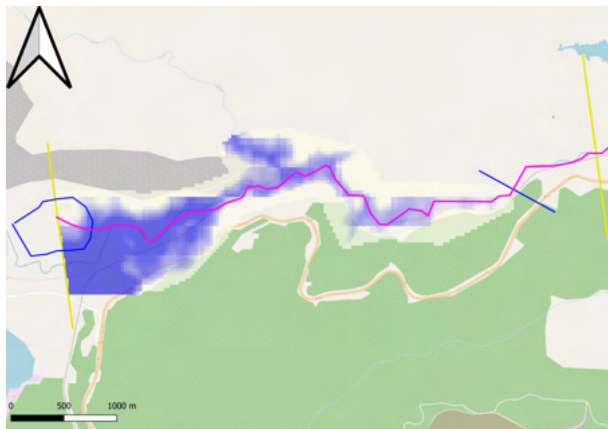
4. SUL SUPERIOR



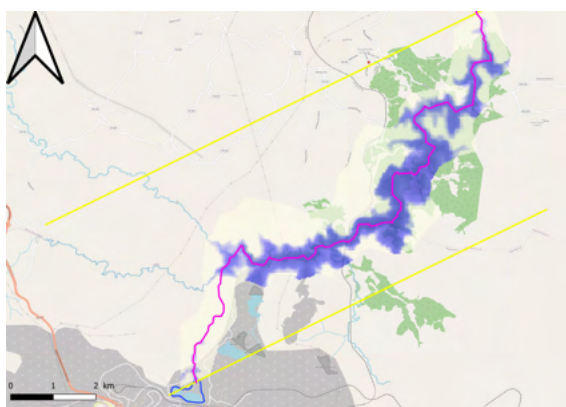
5. FORQUILHA III



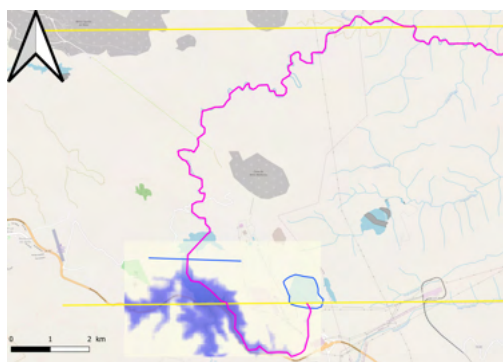
6. DOUTOR



7. ED XINGU



8. GRUPO



9. VARGEM GRANDE

LIST OF SYMBOLS AND ABBREVIATIONS

ANA: Agência Nacional de Águas

ANEEL: Agência Nacional de Energia Elétrica

ANM: Agência Nacional de Mineração

CRI: Risk level

D_{max}: Run-out distance

DTM: Digital Terrain Model

FEAM: Fundação Estadual do Meio Ambiente

H: Elevation difference

H_p: Variable for the potential energy

IMAC: Instituto de Meio Ambiente do Acre

IPAAM: Instituto de Proteção Ambiental do Amazonas

L: Total travelled distance

m.s.l.: mean sea level

PDA: Potential damage associated

TSF: Tailing Storage Facilities

V: Volume of the mass

V_c: Hazard level

V_f: Total volume

V_r: Volume of the reservoir

V_i: Impounded volume

α : Angle of reach

ÍNDICE REMISSIVO

SÍMBOLOS

7 12, 30

A

Agrometeorologia 60

Alto do Cabo Frio 144, 145, 146, 153

Análise Ambiental 10, 1, 11, 48, 49

Análise Instrumental 129, 131, 133, 134, 141, 142, 143

Anomalia magnética 144, 147, 148, 149, 151, 152

Anos Finais do Ensino Fundamental 10, 12, 13, 14, 16, 30

Antioxidantes Naturais 117, 125, 126, 192

Aprendizagem Colaborativa Suportada por Computador 32, 34

Aquífero Bambuí 93, 94, 97, 103, 105, 106, 108

B

Barragem 224, 229, 241, 260

Batimetria 221, 224

Biodiesel 11, 12, 117, 118, 119, 120, 121, 122, 123, 124, 125, 126, 127, 128, 190, 191, 192, 193, 194, 195, 198, 201

C

Canhão eletromagnético 111, 112, 113, 115

Código Python 161

Construção de fotocolorímetros 129

Contextualização 12, 16, 18, 33, 34, 37, 207, 209, 210, 212, 213, 214, 215

Covid-19 11, 86, 87, 89, 90

Cuenca Hidrográfica 74, 75, 76, 77

D

DEM 74, 76, 77, 78, 81, 82, 83

Drones 1, 2, 3, 6, 10

E

Educação Contextualizada 32

Ensino de Ciências 12, 13, 17, 30, 141, 142, 206, 207, 209, 218, 315

Ensino de Física 13, 13, 14, 16, 29, 30, 207, 219, 275, 276, 281, 282, 294, 301

Ensino de Matemática 161, 315

Estabilidade Oxidativa 117, 120, 122, 125, 126, 127, 190

Experimentos 21, 25, 26, 27, 28, 130, 131, 139, 212, 236, 237, 276, 277, 278, 279, 281, 294, 297, 298, 300, 301, 302

Expressões Algébricas 13, 202, 203, 204, 205, 206

F

Fragilidade Ambiental 47, 50, 51, 52, 54, 56, 57, 58, 59

Frequências de Varrição 156

G

Geoprocementos 74, 77, 82

Geotecnologias 1, 2, 5, 47, 49, 50, 56, 157

Gerenciamento 34, 37, 42, 43, 57, 94, 95, 241, 271

Gestão Ambiental 48, 57, 106, 264

I

Imagens de satélite 2, 53, 60, 61

Impactos ambientais 5, 179, 264, 265, 266, 268, 269, 271, 272, 273, 308, 313

Injustiça social 93

Instrumentação com Arduino 275

L

Laboratório Remoto 32, 34, 36, 37, 38, 39, 44

M

Modelagem 12, 142, 176, 179, 190, 192, 224, 286, 292

Modelo Analítico 283, 285, 286, 287, 288, 290, 291

N

Nitrato 93, 94, 104, 105, 106, 107

Nível d'água 221, 224, 234

Nível de redução 221

O

Ordenamento Territorial 10, 47, 48, 49, 50, 51, 52, 54, 55, 56, 57, 58

P

Pandemia 86, 87, 88

Período de Indução 117, 120, 121, 190, 191, 193, 194, 201

Pesquisa documental 207

Potencial Geológico 283

Pressões anormais 13, 236, 237, 239

Processamento Geográfico 156

Programação de Computadores 32, 33, 34, 35, 44

R

Rancimat 117, 118, 120, 122, 126, 193

Receita culinária 202, 205

Recursos didáticos 207

Redes Neurais 57, 191, 192, 193, 195, 198, 199, 200, 201

Resíduos Sólidos 99, 100, 108, 264, 265, 267, 270, 271, 273, 274

Risco 27, 48, 91, 105, 177, 215, 241, 305, 308

Rupturas 241

S

Saneamento 11, 92, 93, 94, 95, 96, 97, 98, 99, 100, 102, 103, 106, 107, 108, 109, 110, 245, 259, 274

Sazonalidade 68, 176

Sensores de baixo custo 13, 275

Sensoriamento Remoto 1, 2, 4, 5, 11, 58, 59, 60, 61, 62, 72, 73, 159, 308, 313

SIG 2, 10, 49, 50, 63, 74, 157, 159, 310

Sistema de Informação Geográfica 156, 157, 310

Smartphones 294, 295, 296, 297, 298, 300, 301, 302

Solenóide 111, 112, 113, 114, 115, 116

Suscetibilidade 12, 49, 151, 176, 178, 179, 182, 183, 188

T

Tectonoestratigrafia 144

Teledetección 74

Termodinâmica 10, 12, 13, 15, 19, 20, 22, 30, 278

Teste de Primalidade 161, 164, 166, 172

TMI e TMIN 93, 106

Trocadores de calor solo-ar (TCSA) 283

V

Vazamentos de óleo 176, 179

Vulcânico 144, 145, 153

Conhecimentos pedagógicos e conteúdos disciplinares

das ciências exatas e da terra



Conhecimentos pedagógicos e conteúdos disciplinares

das ciências exatas e da terra

